2021-10

Cross-sectional flattening-induced nonlinear damped vibration of elastic tubes subjected to transverse loads

Zhu, J

10.1016/j.chaos.2021.111273
Chaos, Solitons and Fractals
Elsevier

Journal: Chaos, Solitons and Fractals:
Article accepted for publication: 12 Jul 2021
Article published online available: 22 Jul 2021
Published online: https://doi.org/10.1016/j.chaos.2021.111273

Cross-sectional flattening-induced nonlinear damped vibration of elastic tubes subjected to transverse loads

Jue Zhu[1], Wei-bin Yuan[2*], Long-yuan Li[3]

[1]*Key Laboratory of Impact and Safety Engineering (Ningbo University) of Ministry of Education, Ningbo, China.*
[2]*College of Architecture and Civil Engineering, Zhejiang University of Technology, Hangzhou, 310023, China.*
[3]*School of Engineering, Computing and Mathematics, University of Plymouth, Plymouth PL4 8AA, UK.*
(* corresponding author)

Abstract - This paper presents an analytical solution of the cross-sectional flattening-induced nonlinear vibration of elastic tubes when subjected to transverse harmonic excitation. It is shown that the equation of motion describing the beam-type transverse vibration of elastic tubes can be characterized by the Duffing equation with cubic nonlinearity, in which the nonlinear term reflects the influence of the cross-sectional flattening on the beam-type transverse vibration of the tubes. The degree of nonlinearity of the transverse vibration is found to be governed directly by the dimensionless amplitude of the harmonic force. The nonlinear feature and corresponding stability of the beam-type response of the tubes under the action of harmonic excitation are discussed. Numerical examples are provided to demonstrate the rationality of the present analytical model.

Keywords: Tubes; nonlinear vibration; ovalization; cross-sectional flattening; beams; cylindrical shells.

1. Introduction

Circular tubes have been widely used in civil, offshore and aerospace engineering. To know the dynamic behavior of circular tubes is very important, particularly when they are working in a dynamic environment. There is a growing appreciation of the importance of nonlinear effects in determining the stability and response of thin-walled shells under the action of dynamic loadings. In general, there are two types of nonlinearities involved in structural analyses, namely the geometric nonlinearity and material nonlinearity. The former is due to the large displacements and thus there is a need to consider the nonlinear relation between the strains and displacements; whereas the latter is due to the stresses which exceed the yield strength of the material and thus there is a need to considers the nonlinear relations between the stresses and strains and/or the plasticity of the material. For many shell structures the deflection, that is the displacement component normal to the shell surface, may be of the order of shell thickness, in which case the nonlinear terms in the strain-displacement relations may

be no longer negligible, as is demonstrated in the buckling analysis of cylindrical shells under axial compression [1] and the flexural vibration analysis of thin-walled circular cylinders [2].

It is noted that the vibration of circularly cylindrical shells normally exhibits multi-half wave modes in their longitudinal and circumferential directions. However, if the shells are long, such as the thin-walled beams of circular hollow section and the beam-type tubes, their low-frequency vibration modal would be dominated by the single half-wave along their longitudinal axis and the ovalization in their cross section [3,4], in which case their nonlinear vibration analysis can be simplified and performed by using the beam-like model but the bending rigidity needs to be modified based on the flattened cross-section.

The cross-sectional ovalization-induced nonlinear deformation in circular tubes and/or circularly cylindrical shells was first reported by Brazier [5] in 1927, who discovered that when a cylindrical shell was bent uniformly, it also flattened its cross-section. Following Brazier's pioneer work, many researchers have studied the influence of cross-sectional ovalization on the static bending response of cylindrical shells. For example, Reissner [6] examined the finite bending of pressured tubes. Aksel'rad [7] presented an analytical study on the upper critical bending load of pipes. Fabian [8], Aksel'rad and Emmerling [9] examined the collapse loads of elastic circular tubes under different types of loadings. Libai and Bert [10], Li [11], and Tatting et al. [12] investigated the nonlinear bending problems of orthotropic composite cylindrical shells. Li and Kettle [13] examined the nonlinear bending response and corresponding nonlinear buckling of ring-stiffened cylindrical shells of finite length under pure bending. Karamanos [14] and Rotter et al. [15] studied the nonlinear stability of thin-walled elastic cylinders of different lengths under global bending. Sato and Ishiwata [16] analyzed the nonlinear response and corresponding Brazier limit-moment of single- and double-walled elastic tubes under pure bending. Xu et al. [17] investigated the nonlinear elastic stability of elliptically cylindrical shells under uniform bending. Coman [18] examined the bifurcation instabilities of circularly cylindrical shells under the action of bending loads. Fajuyitan et al. [19] investigated the nonlinear elastic behavior of short cylindrical shells under global bending. Luongo et al. [20] presented an analytical study on the Brazier effect of elastic pipe beams with foam cores. The results they obtained were validated using finite element analysis results.

The above literature survey shows that there are numerous studies on the cross-sectional ovalization-induced nonlinear behavior of cylindrical shells when subjected to static loads, but very few researches come from the dynamic characteristics of the cylindrical shells. In this paper, the nonlinear dynamic response of elastic circular tubes when subjected to transverse harmonic excitation is studied. The nonlinearity considered in this study is induced by the cross-sectional flattening generated during the beam-type transverse vibration of the tubes. The governing equation describing the beam-type transverse vibration of the tubes with flattened cross-section is derived. The nonlinear feature and corresponding stability of the nonlinear response of the tubes under the action of harmonic excitation are discussed in detail.

2. Vibration equation of elastic circular tubes with cross-sectional flattening

Consider a long, elastic circular tube of length l and mean radius R (see Fig.1) subjected to a transverse harmonic excitation that is uniformly distributed along the longitudinal axis of the tube. When the tube vibrates in the transverse direction, the tensile and compressive longitudinal stresses on opposite sides of the neutral plane combine with the curvature of the longitudinal axis of the tube to flatten its cross-section into an oval shape. Thus the response

of the tube can be characterized by the longitudinal bending deformation (beam-type curvature) and the cross-section bending deformation (ovalization). Let x be the longitudinal axis of the tube, y and z be the transverse and lateral axes on the cross-section of the tube, respectively. According to the two-stage assumption for the deformation made in Brazier approach [5], the transverse vibration of the tube can be described by the deflection function of the tube in the y-direction using the vibration equation of beam-type, whereas the ovalization of cross-section can be taken into account by modifying the bending rigidity of the tube based on the flattened cross-section. In this case the equation of the motion of the elastic circular tube can be expressed as follows,

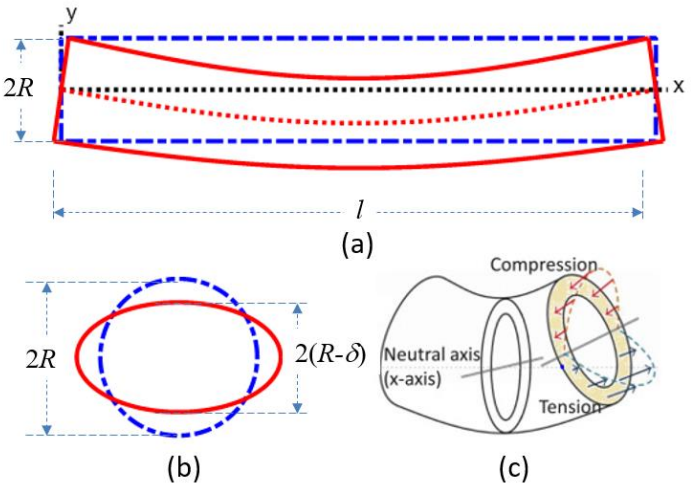

Fig.1 (a) Transverse vibration of simply supported circular tube. (b) Cross-sectional ovalization (blue dash-dot and red solid lines represent un-deformed and deformed shapes). (c) A schematic of deformed tube.

$$m\frac{\partial^2 v}{\partial \tau^2} + c\frac{\partial v}{\partial \tau} + \frac{\partial^2 M}{\partial x^2} = p\cos(\omega_f \tau) \tag{1}$$

where m is the mass of the tube per-unit length, v is the beam-type transverse displacement function of the tube, τ is the time, c is the damping coefficient per unit length, M is the internal bending moment, p and ω_f are the amplitude and frequency of the externally applied harmonic force, respectively. According to the bending theory of beams, the internal bending moment can be expressed in terms of the transverse displacement function as follows,

$$M = EI_z\frac{\partial^2 v}{\partial x^2} \tag{2}$$

where E is the Young's modulus and I_z is the second moment of area of the tube. When the cross-sectional ovalization is considered, the second moment of area of the flattened cross-section is dependent on the transverse bending curvature of the deformed tube [5,11,21]. The larger the curvature, the more serious the flattening. Mathematically, this can be approximately expressed as follows [5,11,21],

$$I_z = I_o\left(1 - \frac{3}{2}\frac{\delta}{R}\right) = I_o\left[1 - \frac{3(1-\nu^2)}{2}\left(\frac{R^2}{h}\frac{\partial^2 v}{\partial x^2}\right)^2\right] \tag{3}$$

where $I_o=\pi hR^3$ is the second moment of area of the undeformed tube, h is the thickness of the tube, R is the mean radius of the tube, δ is the flattening deformation of the cross-section of the tube which is the function of the transverse displacement function v(x), and ν is the Poisson ratio. The detailed derivation of Eq.(3) can be found in [21]. Substituting Eqs.(2) and (3) into (1), it yields,

$$m\frac{\partial^2 v}{\partial \tau^2}+c\frac{\partial v}{\partial \tau}+EI_o\frac{\partial^2}{\partial x^2}\left[\frac{\partial^2 v}{\partial x^2}\left(1-\frac{3(1-\nu^2)}{2}\left(\frac{R^2}{h}\frac{\partial^2 v}{\partial x^2}\right)^2\right)\right]=p\cos(\omega_f\tau) \tag{4}$$

Eq.(4) represents the nonlinear equation of forced vibration of elastic circular tubes under the action of a transverse harmonic excitation. Note that Eq.(4) combines the features of the beam and shell since its longitudinal bending response is promoted based on the bending theory of beams but its cross-sectional flattening response is induced by the circumferential bending in terms of the framework of shells.

For a simply supported circular tube at its two ends (see Fig.1) the low-frequency modal describing the beam-type transverse vibration of the tube can be expressed as,

$$v(\tau,x)=y(\tau)h\sin\frac{\pi x}{l} \tag{5}$$

where y(τ) is a dimensionless function of time, and l is the length of the tube. Substituting Eq.(5) into (4) and then applying Galerkin method to eliminate sin(πx/l) terms on both sides of the equation, it yields,

$$m\frac{d^2 y}{d\tau^2}+c\frac{dy}{d\tau}+EI_o\left(\frac{\pi}{l}\right)^4 y\left[1-\frac{9(1-\nu^2)}{8}\left(\frac{\pi R}{l}\right)^4 y^2\right]=\frac{4p}{\pi h}\cos(\omega_f\tau) \tag{6}$$

Eq.(6) is the nonlinear vibration equation of single degree-of-freedom, which represents the beam-type transverse vibration of the tube when subjected to transverse harmonic excitation, in which the nonlinearity is induced due to the flattening of the cross-section. For the convenience of presentation, the following parameters are introduced,

$$\omega_n=\left(\frac{\pi}{l}\right)^2\sqrt{\frac{EI_o}{m}}\text{ = natural frequency} \tag{7}$$

$$\Omega=\frac{\omega_f}{\omega_n}\text{ = frequency ratio} \tag{8}$$

$$\xi=\frac{c}{2m\omega_n}\text{ = damping ratio} \tag{9}$$

$$\alpha=\frac{9(1-\nu^2)}{8}\left(\frac{\pi R}{l}\right)^4\text{ = coefficient of nonlinear term} \tag{10}$$

$$\beta=\frac{4pl^4}{\pi^5 hEI_o}\text{ = normalized amplitude of externally applied harmonic force} \tag{11}$$

$$t=\omega_n\tau\text{ = dimensionless time} \tag{12}$$

By using the above dimensionless parameters, Eq.(6) can be simplified as follows,

$$\frac{d^2y}{dt^2} + 2\xi\frac{dy}{dt} + y(1-\alpha y^2) = \beta\cos(\Omega t) \tag{13}$$

Further, let $\eta(t) = \sqrt{\alpha}y(t)$ and $f = \sqrt{\alpha}\beta$ where η is the dimensionless response function and f is dimensionless amplitude of the externally applied harmonic force. Eq.(13) becomes,

$$\frac{d^2}{dt^2}\left(\frac{\eta}{f}\right) + 2\xi\frac{d}{dt}\left(\frac{\eta}{f}\right) + \left(\frac{\eta}{f}\right)\left[1 - f^2\left(\frac{\eta}{f}\right)^2\right] = \cos(\Omega t) \tag{14}$$

or

$$\frac{d^2\eta}{dt^2} + 2\xi\frac{d\eta}{dt} + \eta(1-\eta^2) = f\cos(\Omega t) \tag{15}$$

Eq.(14) or (15) is the well-known Duffing equation with cubic nonlinearity [22], for which no exact solution is available in literature. Numerical and/or approximate solutions can be obtained for such a nonlinear second-order differential equation, but their accuracy generally depends on the degree of the nonlinearity of the equation [23-27]. It can be seen from Eq.(14) that the nonlinear term is controlled by the dimensionless amplitude of the harmonic force, *f*. This is because the larger the dimensionless amplitude of the harmonic force, the greater the flattening of the cross-section, and thus the larger the contribution of the nonlinear term. It can be seen from Eq.(15) that the dimensionless response depends on only three dimensionless parameters; they are the damping ratio, frequency ratio, and dimensionless amplitude of the dynamic force, although the original equation of motion, Eq.(4), involves many parameters such as the dimensions and material properties of the tube, the amplitude and frequency of the externally applied dynamic force. This indicates that, among all of these parameters, only three parameters are independent.

The static bending analysis of the elastic circular tube can be obtained by letting Ω=0 and ignoring the inertia and damping forces in Eq.(15), which gives

$$\eta(1-\eta^2) = f \tag{16}$$

The above quadratic algebraic equation describes the relationship between the dimensionless force *f* and the dimensionless displacement η for the case where the load is applied statically. It can be seen from Eq.(16) that the dimensionless force increases with the dimensionless displacement until it reaches to a limit point. After the limit point the dimensionless forces decreases with the increased dimensionless displacement. The critical dimensionless force f_{cr} and corresponding critical dimensionless displacement z_{cr} at the limit point can be calculated from Eq.(16) directly, which gives $f = f_{cr} = 2/(3\sqrt{3})$ and $\eta = z_{cr} = 1/\sqrt{3}$. At the limit point the tube has a limit-point type of instability. By using Eqs.(5) and (11) the static critical load at the limit-point can be calculated from f_{cr} which gives p_{cr}=9.264$ER(t/l)^2$. This critical load is identical to that shown in [21] when the first-order nonlinear term is used. It is also indicated from the obtained static critical load that in the dynamic analysis the dimensionless amplitude of harmonic force should be $f < f_{cr}$.

3. Nonlinear response and stability of elastic circular tubes under transverse harmonic excitation

Fig.2 shows the transverse displacement response of the tube to the harmonic excitation. The solution of Eq.(15) is obtained numerically for the case of ξ=0.2, Ω=0.2, and f=0.8f_{cr} with both initial displacement and initial velocity being assumed to be zero. For the purpose of comparison the linear solution of Eq.(15) is also superimposed in the figure. It can be observed from the figure that the steady-state response of the nonlinear solution is not sinusoidal although the period of the nonlinear response is almost the same as that of the linear response. Fig.3 shows the phase portrait of the linear and nonlinear responses. It is obvious from the figure that, unlike the linear solution which exhibits elliptical shape after it reaches to steady-state, the shape of the steady-state nonlinear solution seems rather complicated. Also it can be found from Figs.2 and 3 that the amplitude of the nonlinear response is larger than that of corresponding linear response due to the influence of stiffness softening generated by the cross-sectional flattening. Herein, it should be mentioned that the 20% damping ratio employed in this example is quite large. If a small damping ratio were used the difference between the obtained linear and nonlinear solutions would be even bigger. There is an increasingly interest in literature on the nonlinear vibration and dynamic stability of beams, particularly for beams made from composites such as carbon nanotube-reinforced composite micro-beams [28-32].

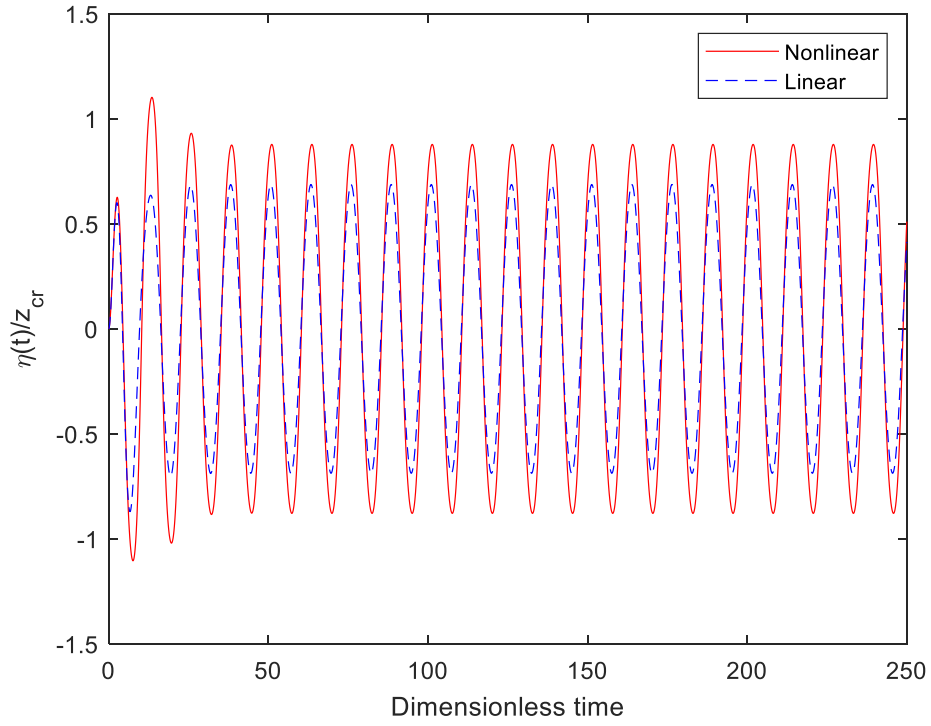

Fig.2 Comparison of linear and nonlinear responses (ξ=0.2, Ω=0.2 and f=0.8f_{cr}).

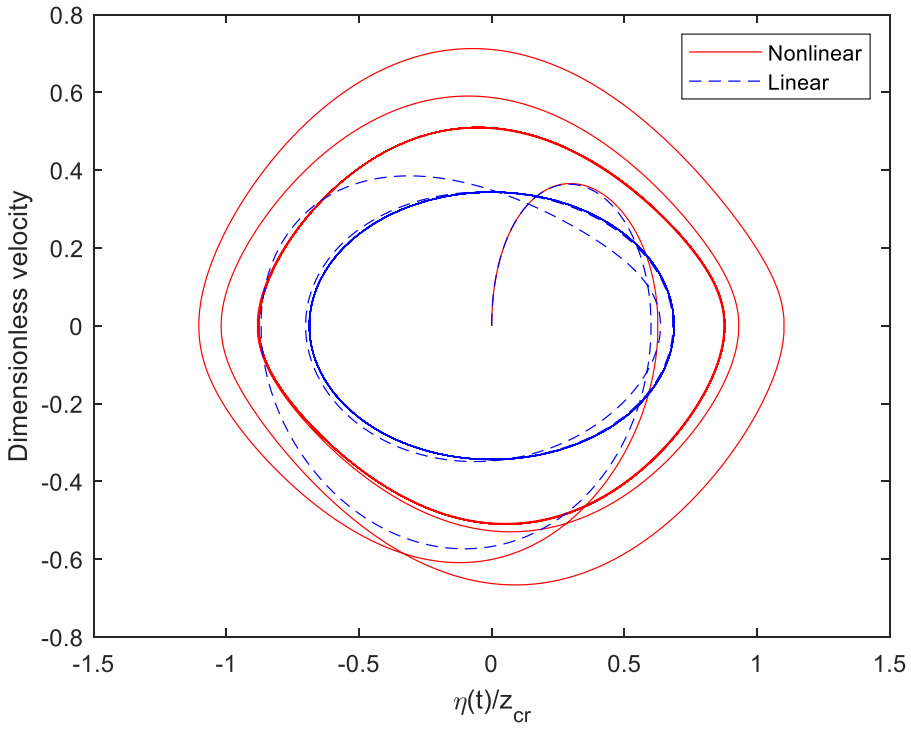

Fig.3 Comparison of phase portraits of the linear and nonlinear responses (ξ=0.2, Ω=0.2 and f=0.8f_{cr}).

In order to investigate the stability of the dynamic system described by Eq.(15), an analytical approximate solution of Eq.(15) needs to obtain first. Jiang et al. [33] made a comparison on various different approximate methods used for solving nonlinear forced vibration equation. It is shown that the harmonic balance method [23] is more effective to give comprehensive nonlinear features and thus is employed herein, although other methods could also be used [34-36]. As an approximation, the following solution for Eq.(15) is assumed,

$$\eta(t) = a\cos(\Omega t) + b\sin(\Omega t) \tag{17}$$

where a and b are the constants to be determined. Substituting Eq.(17) into (16), it yields,

$$\begin{aligned}&\left(-\Omega^2 a + 2\xi\Omega \mathrm{b} + a - \tfrac{3}{4}a^3 - \tfrac{3}{4}ab^2 - f\right)\cos(\Omega t)\\ &\quad -\left(\Omega^2 b + 2\xi\Omega a - b + \tfrac{3}{4}b^3 + \tfrac{3}{4}a^2 b\right)\sin(\Omega t)\\ &-\left(\tfrac{1}{4}a^3 - \tfrac{3}{4}ab^2\right)\cos(3\Omega t) - \left(\tfrac{3}{4}a^2 b - \tfrac{1}{4}b^3\right)\sin(3\Omega t) = 0\end{aligned} \tag{18}$$

By ignoring the super-harmonics at 3Ω, the two terms preceding cos(Ωt) and sin(Ωt) have to be zero. As a result of this, we have,

$$\Omega^2 a - 2\xi\Omega \mathrm{b} - a + \tfrac{3}{4}(a^2 + b^2)a = f \tag{19}$$

$$\Omega^2 b + 2\xi\Omega a - b + \frac{3}{4}(a^2 + b^2)b = 0 \qquad (20)$$

Let $z = \sqrt{a^2 + b^2}$ be the amplitude of η(t). By squaring both sides of Eqs. (19) and (20), then adding the two equations together, it yields,

$$z = \frac{f}{\sqrt{\left(1-\Omega^2-\frac{3}{4}z^2\right)^2+(2\xi\Omega)^2}} \qquad (21)$$

Eq.(21) provides the relationship between the frequency ratio Ω, damping ratio ξ, dimensionless amplitude f of the harmonic force, and dimensionless amplitude z of the nonlinear response of the dynamic system described by Eq.(15) when the nonlinearity is not very strong. It is obvious that if the nonlinear term of $(3z^2/4)$ in the denominator of Eq.(21) is ignored, Eq.(21) reduces to the dimensionless amplitude of the linear response. Eq.(21) can be used to determine (1) the relationship between the force-amplitude and displacement-amplitude for given frequency ratio and damping ratio and (2) the relationship between the frequency ratio and displacement-amplitude for given force-amplitude and damping ratio.

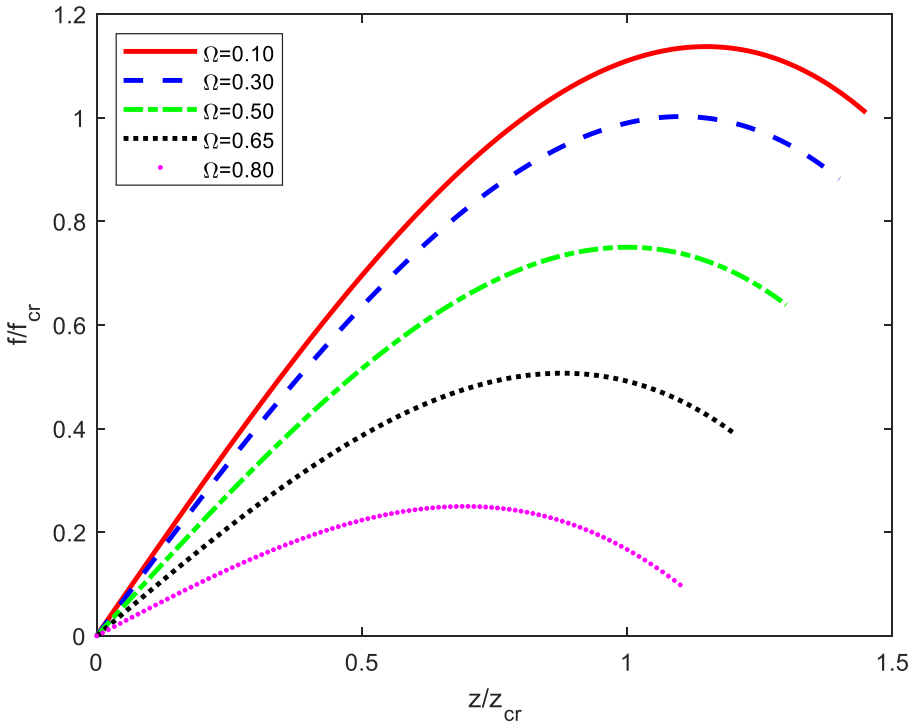

(a)

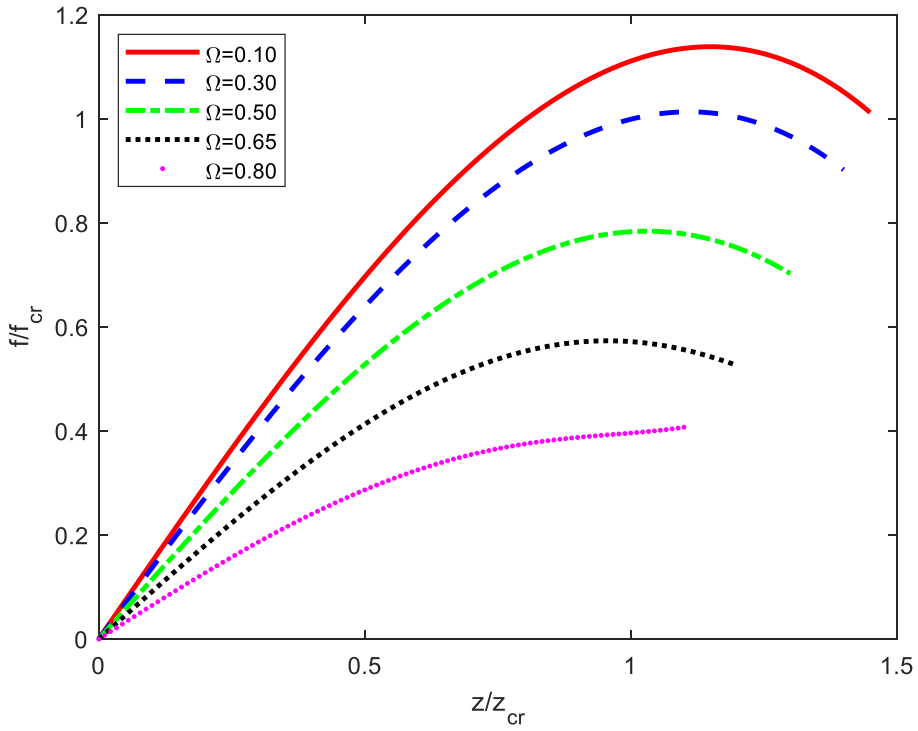

(b)

Fig.4 Force-amplitude versus displacement-amplitude for different frequency ratios. (a) ξ=0.01 and (b) ξ=0.15.

Fig.4 shows the variation of the force amplitude with the displacement amplitude for various different frequency ratios calculated from Eq.(21). Fig.4a is for the damping ratio of 1.0% and Fig.4b is for the damping ratio of 15%. It can be seen from the figure that, due to the nonlinearity induced by the flattening of cross-section, the relationship between the force amplitude and displacement amplitude is not linear and there exists a peak point in the curve except for the case where both the damping ratio and frequency ratio are high (Ω=0.8, ξ=0.15). After the peak point the force amplitude decreases with increased displacement amplitude, which represents the post-buckling of the tube after it has a snap-through dynamic instability. The force amplitude at the peak point represents the limit load which the tube can carry. It can be found from Fig.4 that, when the frequency ratio increases the corresponding limit load reduces; indicating the influence of the force frequency on the dynamic instability of the elastic circular tubes. Also, it can be seen from the figure that when the damping ratio increases the limit load increases marginally and the curve near the limit-point becomes more flattened; indicating that there is weak nonlinearity.

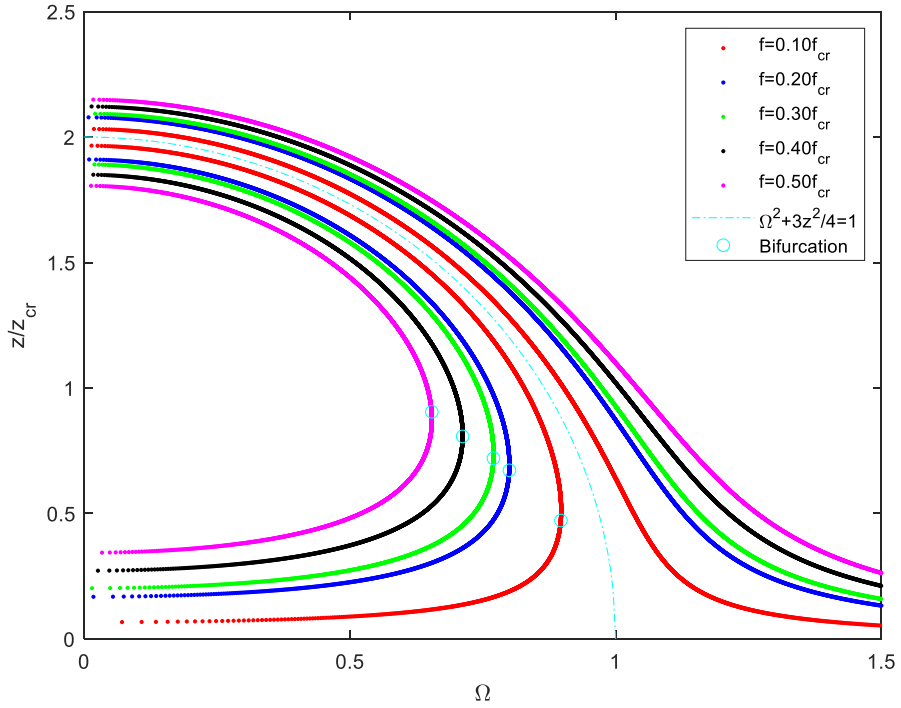

(a)

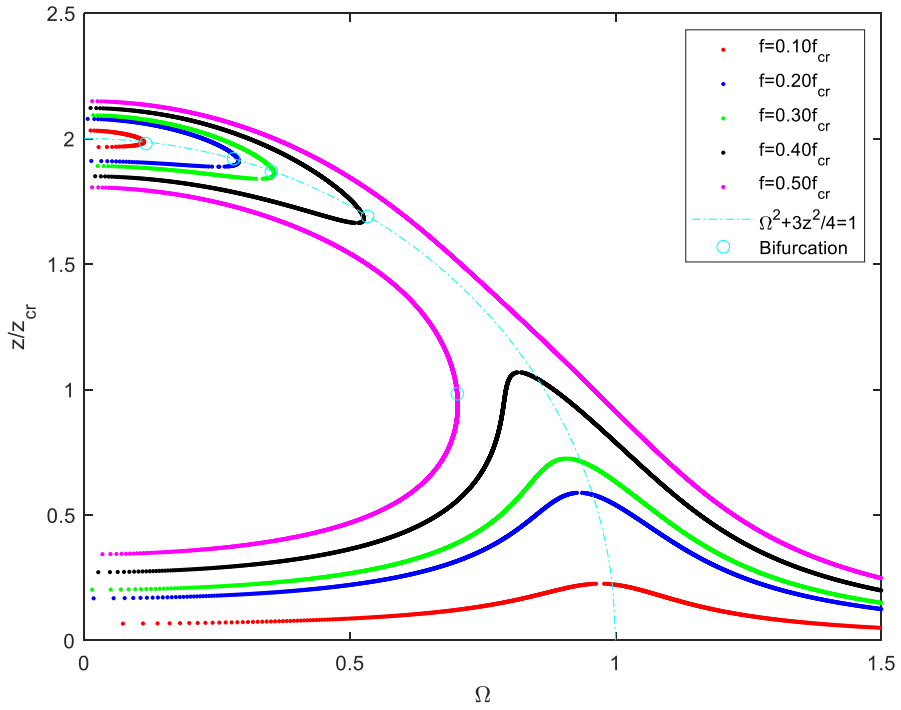

(b)

Fig.5 Amplitude-frequency response. (a) ξ=0.01 and (b) ξ=0.15.

Fig.5 shows the amplitude-frequency responses calculated using Eq.(21) for five different force-amplitudes at two damping ratios (ξ=0.01, ξ=0.15). Unlike the case of a linear system where an amplitude corresponds to only a frequency ratio and the amplitude-frequency response is linearly proportional to the force-amplitude, in the nonlinear system, however, it is possible that more than one amplitudes correspond to a frequency ratio and the influence of the force-amplitude on the amplitude-frequency response is rather complicated. It can be seen from the figure that for a given force-amplitude the amplitude-frequency response contains two separate curves; one of which covers all frequency ratios (named as main curve), the other of which covers only part of the frequency ratios (named as trivial curve). When the damping ratio is small (see Fig.5a for ξ=0.01) the main curve and trivial curve are separated by the locus defined by the equation of $\Omega^2+3z^2/4=1$. For a given Ω value, the trivial curve gives two roots of the amplitude except at the bifurcation point where there is only one root; whereas the main curve gives only one root of the amplitude for a given Ω value. At the bifurcation point the amplitude will jump from the main curve to the trivial curve or vice versa, which represents the dynamic snap-through instability and thus the frequency ratio and corresponding force-amplitude at the bifurcation point can be considered as the critical frequency and critical dynamic load.

When the damping ratio is large (Fig.5b for ξ=0.15) the amplitude-frequency response is heavily dependent on the value of the force-amplitude. For small and medium force-amplitudes (f=0.1f_{cr} to f=0.4f_{cr}) the peak amplitude point in the main curve is found to move upward and bends toward to the left as the excitation amplitude is increased; whereas the bifurcation point at the trivial curve moves to right and bends downwards. The vibration feature is largely characterized by the linear vibration in the main curve and by the nonlinear vibration in the trivial curve. With the increase in force-amplitude, the peak amplitude point in the main curve and the bifurcation point in the trivial curve merge together. With the further increase in force-amplitude (f=0.5f_{cr}), both the main curve and trivial curve split into two parts at its peak amplitude point or bifurcation point. The two parts above the locus, one from the main curve and one from the trivial curve, join together to form a new main curve; whereas the two parts below the locus, also one from the main curve and one from the trivial curve, join together to form a new trivial curve. Similarly, the bifurcation point located at the old or new trivial curve indicates that the dynamic snap-through instability could occur at that point and thus the frequency ratio and corresponding force-amplitude at that point can be considered as the critical frequency and critical dynamic load.

Fig.6 shows the influence of damping ratio on the amplitude-frequency response, calculated using Eq.(21) for a fixed force-amplitude of f=0.5f_{cr}. For the purpose of comparison, the results obtained from the linear dynamic analysis are also superimposed in the figure. It can be seen from the figure that, the difference in the results between the linear and nonlinear analyses decreases with the increase of damping ratio. For the case where the damping ratio is ξ=0.3, the results obtained from the linear and nonlinear analyses have almost no difference in their main curves. Also, it can be observed from the figure that the damping ratio has a significant effect on the amplitude-frequency response. For example, under the excitation of f=0.50f_{cr}, the response will have a dynamic snap-through instability at Ω=0.65 and Ω=0.70 when the damping ratio equals to 0.01 and 0.15, respectively. However, under the same excitation, if the damping ratio increases to 0.30, the dynamic instability will occur at Ω=0.29, which is much less than other two frequency ratios.

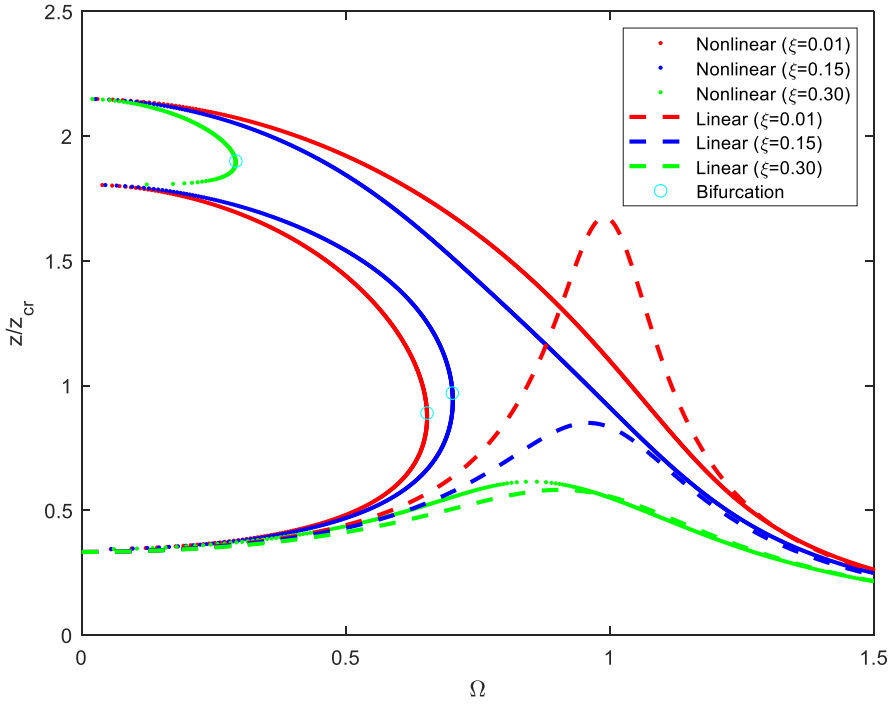

Fig.6 Amplitude-frequency response (f=0.50f_{cr}).

4. Conclusions

This paper has presented an analytical study on the nonlinear transverse vibration of elastic circular tubes when subjected to transverse excitations induced by the cross-sectional flattening. From the results obtained the following conclusions can be drawn:

- A generalized nonlinear transverse vibration equation for elastic circular tubes has been derived which is represented by using dimensionless parameters. The degree of nonlinearity of the transverse vibration of elastic circular tubes is found to be governed by the dimensionless amplitude of the harmonic force.
- The nonlinear equation of motion characterizing the beam-type transverse vibration of elastic circular tubes induced by the cross-sectional flattening can be represented by the Duffing equation with a cubic nonlinear term.
- The limit-point load describing the dynamic snap-through instability can be calculated using Eq.(21) and the influence of frequency ratio and damping ratio on the limit-point load can be also evaluated using Eq.(21).
- The amplitude-frequency responses obtained from Eq.(21) are able to explain the feature of dynamic bifurcation and/or dynamic instability of elastic circular tubes. It is found that the damping ratio has a significant influence on the dynamic bifurcation and dynamic instability of elastic circular tubes.

Declaration of interests - The authors declare that they have no known competing financial interests or personal relationships that could have appeared to influence the work reported in this paper.

Acknowledgment - The first author would like to acknowledge the financial support received from National Natural Science Foundation of China (No.11572162 and No.11972203), Ningbo Municipal Natural Science Foundation (No. 202003N4152), Ningbo Special Equipment Inspection Institute, Ningbo Rail Transit (JS-00- SG-17003), and K.C. Wong Magna Fund at Ningbo University for their financial support.

References

[1] von Karman T, Tsien HS. The buckling of thin cylindrical shells under axial compression. J. Aeronautical Sci. 1941; 8(8): 303-312.
[2] Chu HN. Influence of large amplitudes on flexural vibrations of a thin circular cylindrical shell. J. Aerospace Sci. 1961; 28(8): 602-609.
[3] Birman V, Bert CW. Non-linear beam-type vibrations of long cylindrical shells. International Journal of Non-Linear Mechanics 1987; 22(4): 327-334.
[4] Molyneaux CK, Li LY. Dynamic elastic instability of long circular cylindrical shells under pure bending. Thin-Walled Structures 1996; 24(2): 123-133.
[5] Brazier LG. On the flexture of thin cylindrical shells and other thin sections. Proc. R. Soc. Ser. A 1927; 116(773): 104–111.
[6] Reissner E. On finite bending of pressured tubes. J. Appl. Mech. (ASME) 1959; 26: 386–392.
[7] Aksel'rad EL. Pinpointing the upper critical bending load of a pipe by calculating geometric nonlinearity. Izv. Akad. Nauk SSR Mekh. 1965; 4: 133–139.
[8] Fabian O. Collapse of cylindrical elastic tubes under combined bending, pressure and axial loads. Int. J. Solids Struct. 1977; 13(12): 1257– 1270.
[9] Aksel'rad EL, Emmerling FA. Collapse load of elastic tubes under bending. Isr. J. Technol. 1984; 22: 89–94.
[10] Libai A, Bert CW. A mixed variational principle and its application to the nonlinear bending problem of orthotropic tubes—II. Application to nonlinear bending of circular cylindrical tubes. Int. J. Solids Struct. 1994; 31(7): 1019–1033.
[11] Li LY. Bending instability of composite tubes. J. Aerospace Eng. (ASCE) 1996; 9(2) 59–61.
[12] Tatting BF, Gurdal Z, Vasiliev VV. The Brazier effect for finite length composite cylinders under bending. Int. J. Solids Struct. 1997; 34(12): 1419–1440.
[13] Li LY, Kettle R. Nonlinear bending response and buckling of ring-stiffened cylindrical shells under pure bending. International Journal of Solids and Structures 2002; 39(3): 765-781.
[14] Karamanos S. Bending instabilities of elastic tubes, Int. J. Solids Struct. 2002; 39(8): 2059–2085..
[15] Rotter MJ, Michael S, Adam J, Lei C. Nonlinear stability of thin elastic cylinders of different length under global bending. International Journal of Solids and Structures 2014; 51(15–16): 2826-2839.
[16] Sato M, Ishiwata Y. Brazier effect of single- and double-walled elastic tubes under pure bending, Struct. Eng. Mech. 2015; 53(1): 17–26.

[17] Xu ZY, Gardner L, Sadowski AJ. Nonlinear stability of elastic elliptical cylindrical shells under uniform bending. International Journal of Mechanical Sciences 2017; 128-129: 593-606.
[18] Coman CD. Bifurcation instabilities in finite bending of circular cylindrical shells. Interational Journal of Engineering Science 2017; 119: 249-264.
[19] Fajuyitan OK, Sadowski AJ, Wadee MA, Rotter JM. Nonlinear behaviour of short elastic cylindrical shells under global bending. Thin-Walled Structures 2018; 124: 574-587.
[20] Luongo A, Zulli D, Scognamiglio I. The Brazier effect for elastic pipe beams with foam cores. Thin-Walled Structures 2018; 124: 72–80.
[21] Zhu J, Li LY. Nonlinear bending of cylindrical shells subjected to transverse loads. Mechanics Research Communications 2020; 107: 103561.
[22] Nayfeh AH, Nayfeh JF, Mook DT, On methods for continuous systems with quadratic and cubic nonlinearities. Nonlinear Dynamics 1992; 3: 145-162.
[23] Huseyin K, Lin R. An intrinsic multiple-scale harmonic balance method for nonlinear vibration and bifurcation problems. International Journal of Nonlinear Mechanics 1991; 26(5): 727-740.
[24] Liu QX, Liu JK, Chen YM, An analytical criterion for jump phenomena in fractional Duffing oscillators. Chaos, Solitons & Fractals 2017; 98: 216-219.
[25] Marinca V, Herişanu N. Periodic solutions of Duffing equation with strong non-linearity. Chaos, Solitons & Fractals 2008; 37(1): 144-149.
[26] Zhang G, Wu Z. Homotopy analysis method for approximations of Duffing oscillator with dual frequency excitations. Chaos, Solitons & Fractals 2019; 127: 342-353.
[27] Wang QB, Yang YJ, Zhang X. Weak signal detection based on Mathieu-Duffing oscillator with time-delay feedback and multiplicative noise. Chaos, Solitons & Fractals 2020; 137: 109832.
[28] Jalaei MH, Civalek O. On dynamic instability of magnetically embedded viscoelastic porous FG nanobeam. International Journal of Engineering Science 2019; 143: 14-32.
[29] Dastjerdi S, Akgöz B, Civalek O. On the effect of viscoelasticity on behavior of gyroscopes. International Journal of Engineering Science 2020; 149: 103236.
[30] Civalek O, Dastjerdi S, Akbaş SD, Akgöz B. Vibration analysis of carbon nanotube-reinforced composite microbeams. Mathematical Methods in the Applied Sciences (2020) (https://doi.org/10.1002/mma.7069).
[31] Demir C, Civalek O. On the analysis of microbeams, International Journal of Engineering Science 2017; 121: 14-33.
[32] Akgoz B, Civalek O. Longitudinal vibration analysis for microbars based on strain gradient elasticity theory. Journal of Vibration and Control 2014; 20(4): 606-616.
[33] Jiang W, Zhang G, Chen L. Forced response of quadratic nonlinear oscillator: comparison of various approaches. Applied Mathematics and Mechanics 2015; 36(11): 1403-1416.
[34] Xu P, Wellens P. Effects of static loads on the nonlinear vibration of circular plates. Journal of Sound and Vibration 2021; 504: 116111.
[35] Markakis MP. The jump phenomenon associated with the dynamics of the duffing equation. Physics Open 202; 5: 100042.
[36] Mohamed N, Eltaher MA, Mohamed SA, Seddek LF. Numerical analysis of nonlinear free and forced vibrations of buckled curved beams resting on nonlinear elastic foundations. International Journal of Non-Linear Mechanics 2018; 101: 157-173.